Fungal Biology 124 (2020) 144–154

Contents lists available at ScienceDirect

Fungal Biology

journal homepage: www.elsevier.com/locate/funbio

Genome comparison and transcriptome analysis of the invasive brown root rot pathogen, *Phellinus noxius*, from different geographic regions reveals potential enzymes associated with degradation of different wood substrates

Jorge R. Ibarra Caballero [a], Jessa P. Ata [a, b], K.A. Leddy [a], Travis C. Glenn [c], Troy J. Kieran [c], Ned B. Klopfenstein [d], Mee-Sook Kim [e, **], Jane E. Stewart [a, *]

[a] Department of Bioagricultural Sciences and Pest Management, Colorado State University, Fort Collins, CO 80523, USA
[b] Department of Forest Biological Sciences, University of the Philippines Los Baños, Laguna 4031, Philippines
[c] Department of Environmental Health Science, University of Georgia, Athens, GA 30602, USA
[d] USDA Forest Service, Rocky Mountain Research Station, Moscow, ID 83843, USA
[e] USDA Forest Service, Pacific Northwest Research Station, Corvallis, OR 97331, USA

ARTICLE INFO

Article history:
Received 15 August 2019
Received in revised form
11 December 2019
Accepted 18 December 2019
Available online 8 January 2020

Corresponding Editor: J Slot

Keywords:
Illumina
Invasive forest pathogen
Plant cell wall degrading enzymes
Root decay pathogen
White-rot fungus

ABSTRACT

Phellinus noxius is a root-decay pathogen with a pan-tropical/subtropical distribution that attacks a wide range of tree hosts. For this study, genomic sequencing was conducted on *P. noxius* isolate P919-02W.7 from Federated States of Micronesia (Pohnpei), and its gene expression profile was analyzed using different host wood (*Acer*, *Pinus*, *Prunus*, and *Salix*) substrates. The assembled genome was 33.92 Mbp with 2954 contigs and 9389 predicted genes. Only small differences were observed in size and gene content in comparison with two other *P. noxius* genome assemblies (isolates OVT-YTM/97 from Hong Kong, China and FFPRI411160 from Japan, respectively). Genome analysis of *P. noxius* isolate P919-02W.7 revealed 488 genes encoding proteins related to carbohydrate and lignin metabolism, many of these enzymes are associated with degradation of plant cell wall components. Most of the transcripts expressed by *P. noxius* isolate P919-02W.7 were similar regardless of wood substrates. This study highlights the vast suite of decomposing enzymes produced by *P. noxius*, which suggests potential for degrading diverse wood substrates, even from temperate host trees. This information contributes to our understanding of pathogen ecology, mechanisms of wood decomposition, and pathogenic/saprophytic lifestyle.

1. Introduction

Molecular genetic tools provide a means to obtain in-depth insights into forest ecological dynamics, such as pathogen-tree host interactions and diverse ecological roles of forest-associated fungi. The 'omics' technologies offer high-resolution interpretations ranging from a single pathogen's biological functions to complex ecological interactions that allow more holistic approaches to enhance forest health and ecosystem services (Stewart et al., 2018). Genomics has led to identification of unique and conserved genes that serve as diagnostic tools for rapid screening of plant pathogens (Feau et al., 2018). In forest disease management, for example, monitoring invasive rust pathogens of pines and poplars has become more efficient with real-time PCR assays, based on genome-enhanced detection and identification (Bergeron et al., 2019). Genomic comparisons also help deduce evolutionary mechanisms of effectors and other pathogenicity-related genes among fungal pathogens (Plissonneau et al., 2017). While genomics uncovers the pathogen's genetic potential, transcriptomics provides a glimpse of the pathogen's metabolism as it interacts with its environment (Ross-Davis et al., 2013; Kovalchuk et al., 2019).

Phellinus noxius, the causal agent of the lethal brown root rot disease, affects a wide range of hosts causing substantial losses in

* Corresponding author.
** Corresponding author.
E-mail addresses: meesook.kim@usda.gov (M.-S. Kim), Jane.Stewart@colostate.edu (J.E. Stewart).

https://doi.org/10.1016/j.funbio.2019.12.007
1878-6146/

shade, fruit, ornamental, and plantation trees (Ann et al., 1999; Bolland, 1984; Sahashi et al., 2012, 2014). More than 200 plant species in 59 families throughout Africa, Central America, the Caribbean, Oceania, and Southeast Asia have been reported to be susceptible to this pathogen (CABI, 2018). *P. noxius* can infect host plants of all ages, mostly tree species and a few herbaceous host plants, that are often killed via rapid disease development, as quickly as 6 m in some cases (Ann et al., 1999, 2002). The pathogen can subsist saprophytically for over 10 y (Chang, 1996), but its growth temperature range, 8-36 °C, likely explains the restriction of the pathogen to tropical and subtropical areas (Ann et al., 2002; Chung et al., 2017). Due to the pathogen's geographic extent on continental landforms as well as both oceanic and continental islands, *P. noxius* has been suggested as a model for the evolution of fungal forest diseases on oceanic islands (Akiba et al., 2015).

Levels of genetic polymorphism within *P. noxius* are relatively high across its distribution (Stewart et al., In press). Populations from Japan were found to be highly polymorphic across 20 microsatellite loci suggesting the species' long occurrence in the region (Akiba et al., 2015). Among 91 Taiwanese isolates, three distinct groups were identified based on 20 variable nucleotide sites and variable ITS-sequence lengths (Tsai et al., 2017). Population genomic analysis also revealed abundant variation among isolates from the Asia–Pacific region, particularly Japan and Taiwan (Chung et al., 2017). Alongside potential gene flow and mutation rates, such diversity may be linked to the species' bipolar heterothallic mating system and pre-dominantly outcrossing reproductive mode (Chung et al., 2015, 2017). Although several studies have shown high levels of genetic diversity across populations of *P. noxius*, the relationship of this genetic variation to pathogenicity and wood decomposition is largely unknown.

Wood-decaying Basidiomycota fungi can be classified as either white-rotters, for their ability to degrade all components of plant cell walls (cellulose, hemicellulose, other wood components, and lignin) or brown-rotters, which also degrade cell wall components with the exception of lignin. While *P. noxius* causes the disease known as "brown root rot" due to the black mycelial crust produced by the pathogen on the infected plant surface, it is classified as a white-rot fungus because it is able to degrade lignin (Brooks, 2002). Enzymes involved in lignin degradation include laccases [classed as family 1 of the Auxiliary Activities (AA) in the Carbohydrate Active Enzymes database (CAZy): AA1], lignin-modifying peroxidases (AA2), and enzymes that are necessary to complete the degradation process, such as glyoxal oxidase (AA5), aryl-alcohol oxidase, pyranose oxidase, glucose oxidase, and cellobiose dehydrogenase (AA3), vanillyl alcohol oxidase (AA4) (Janusz et al., 2017; Levasseur et al., 2013), and cytochrome P450 (Ichinose, 2013; Qhanya et al., 2015). Extracellular secretion of these enzymes has been found across many different Basidiomycota fungi (Janusz et al., 2017). Comparative genomic analysis revealed AA2 genes as conserved among white-rot fungi of class Agaricomycetes (Floudas et al., 2012); however, differences in enzyme complements and mechanisms of wood decomposition have been found among different fungal taxa (Janusz et al., 2017; Levasseur et al., 2008; Ohm et al., 2014; Riley et al., 2014; Floudas et al., 2015).

The ability for *P. noxius* to infect a broad host range implies a dynamic gene arsenal to convey pathogenicity. Population genomic analysis of this pathogen showed hypervariability, wherein two distinct lineages with opposing evolutionary scenarios were found, suggesting potential adaptability of the pathogen to various environments (Chung et al., 2017). The high genetic diversity of *P. noxius* and its broad host range offers an opportunity for examining gene expression associated with plant cell wall degradation. We hypothesize that *P. noxius* possesses a large repertoire of variably expressed, wood-degrading enzymes. Evidence supporting this hypothesis was presented in a recent study by Chung et al. (2017), in which carbohydrate-active enzymes (CAZymes), including families of AA lignin-degrading enzymes (AA1-AA9) (e.g., laccases, peroxidases, oxidases, and reductases), were found in the genomes of all Hymenochaetales species examined, including *P. noxius*. To further examine this hypothesis, we report the annotated genome of *P. noxius* isolate P919-02W.7 from Federated States of Micronesia (Pohnpei), and evaluate the gene content and gene expression on various host wood substrates using transcriptomics. To assess genomic differences among *P. noxius* from different geographic origins, we also compare genomic characteristics and gene content of isolate P919-02W.7 (Pohnpei) with previously available genomics sequences of isolates, OVT-YTM/97 (Hong Kong, China) and FFPRI411160 (Japan).

2. Material and methods

2.1. Genome sequencing and assembly

Putatively diploid mycelium of *P. noxius* isolate P919-02W.7 was collected beneath the bark of dye fig (nihn; *Ficus tinctorial*) on Pohnpei (ca. N06.82381°; E158.17033°) in September 2013 and established in culture on potato dextrose agar (Stewart et al., In press). This isolate is housed in the Stewart Laboratory at Colorado State University and is available upon request. DNA was extracted using cetyltrimethylammonium bromide (CTAB) extraction protocol similar to Ibarra Caballero et al. (2019). Genomic DNA was submitted to the Georgia Genomics and Bioinformatics Core (GGBC; Athens, GA, USA) for Illumina-compatible library preparation. Two types of libraries were prepared, an Illumina TruSeq short-insert library with 400–450 bp inserts and an Illumina Nextera Mate Pair Library with ~5 kb inserts (Illumina Inc., San Diego, CA, USA). Libraries were sequenced on an Illumina NextSeq at the GGBC to obtain paired-end 150-base (PE150) reads.

For genome assembly, contigs were first generated using paired-end reads in MIRA V.4.0.2. The MIRA contigs were then used as trusted-contigs, along with mate-paired read in Spades-3.10.1 to produce the final assembly. The draft genome assembly of *P. noxius* isolate P919-02W.7 was submitted to NCBI Genbank with accession number VSJA01000000.

The Python package Pyani (https://github.com/widdowquinn/pyani) was used to calculate the average nucleotide identity between the genome assembly of *P. noxius* isolates P919-02W.7 (Pohnpei), compared to OVT-YTM/97 (Hong Kong: Accession # AYOR00000000) and FFPRI411160 (Japan: Accession # NBII00000000), which were downloaded from NCBI GenBank. Three different alignment algorithms used by Pyani, ANIm (that uses NUCmer), ANIb (that uses BLASTN), and TETRA (that calculates tetranucleotide frequencies of each input sequence), were included.

2.2. Genome annotation

MAKER annotation pipeline v.2.31.8 (Cantarel et al., 2008) was used for genome annotation of the three genome assemblies from Pohnpei, Hong Kong, and Japan. A custom set of repetitive sequences was obtained using RepeatModeler v.1.0.11 (Smit and Hubley, 2017) and used by RepeatMasker v.4.0.6 (Smit et al., 2015) to identify and mask interspersed repeats and low complexity DNA sequences. For use as RNASeq evidence in Maker, a draft transcriptome from the wood-degradation experiment (see below under "Transcriptome analysis") for *P. noxius* isolate P919-02W.7 (Pohnpei) was assembled using TopHat v.2.1.1 and Cufflinks v.2.2.1 (Trapnell et al., 2014). For use as protein evidence in Maker, sequences from a set of proteins of Hymenochaetaceae were obtained from the UniProt database. Three gene predictor

programs: SNAP v2013-11-29 (Zaharia et al., 2011), AUGUSTUS v.2.2.3 (Keller et al., 2011), and GeneMark-ES v.4.32 (Ter-Hovhannisyan et al., 2008) were included in the MAKER pipeline. *Laccaria bicolor* was used as species model for AUGUSTUS. Predicted genes smaller than 150 bases long were not considered for further analysis.

Proteins predicted by MAKER were used for functional annotation. BLASTP was run using NCBI-BLAST-2.7.1+ (Camacho et al., 2009) against fungal sequences in the UniProt database, against the PHI database version 45 (Urban et al., 2017), and against the MEROPS release 12.0 database (Rawlings et al., 2018). InterProScan-5.30-69.0 (Jones et al., 2014) was used to search for Pfam motifs in the protein sequences. CAZymes were annotated using the dbCAN web server (http://csbl.bmb.uga.edu/dbCAN/) (Yin et al., 2012). Assignments of the annotated CAZymes to specific substrates were based on information obtained at the Carbohydrate-active enzymes database (Lombard et al., 2014), and the CAZypedia (The CAZypedia Consortium, 2018). Secreted (extracellular) proteins were predicted using the stand-alone version of Deeploc v.1.0 (Almagro Armenteros et al., 2017), a program that uses deep neural networks based on the protein sequence information. Secondary metabolism genes were detected using antiSMASH 4.0 (Blin et al., 2017). Gene Ontology (GO) information was obtained using the Argot 2.5 web server (Lavezzo et al., 2016); only predictions with a total score ≥200 or with internal confidence ≥0.99 and with total score ≥2.0 were kept. Fisher's exact tests, with p-values adjusted for multiple comparisons (Benjamini-Hochberg), were used to compare the number of transcripts in the 15 more abundant transcriptome GO terms to the number of corresponding genes assigned to the same GO terms.

2.3. Transcriptome analysis

To obtain *P. noxius* mycelia for RNA extraction, stem cross sections (ca. 3–4 cm diameter x 1 cm thick) of four woody species [ponderosa pine (*Pinus ponderosa*), mahaleb cherry (*Prunus mahaleb*), black willow (*Salix nigra*), and sugar maple (*Acer saccharum*)] were prepared for inoculation. Autoclave-sterilized stem sections of each species were placed on top of sterile water agar within deep Petri dishes (95 mm diameter x 80 mm high) and three small inoculum pieces (ca. 5 mm × 5 mm) were placed onto the agar. Inoculated stem sections were incubated in growth chamber at 28 ± 2 °C, and mycelia subsequently grew onto the surface of the stem sections. Two replicates for each wood type (tree species), each one consisting of mycelium growing on stem sections within separate petri dishes, were obtained. After 6 weeks, *P. noxius* mycelia were gently removed from the upper stem-section surface using forceps and immediately immersed into 1.0 mL RNA*later*® Stabilization Solution (ThermoFisher Scientific, NY, USA) within 2.0-mL microcentrifuge tubes. The tubes were sealed and maintained at −80 °C until RNA extraction. RNA was extracted using the Qiagen RNeasy® (Qiagen, Germantown, MD, USA) reagents and following the manufacturer protocols with one modification. Samples were lysed with PowerBead Tubes (MoBio Laboratories, Inc., Carlsbad, CA, USA) on a vortexer for 10 min, replacing the buffer with Qiagen RNeasy lysis buffer. RNA elution was performed using two rounds of 30 μL RNA-free H_2O for a final volume of 60 μL. Libraries were then prepared using a KAPA Stranded mRNA-seq kit (KAPA Biosystems, Wilmington, MA, USA) using half–volume reaction sizes and a temperature of 87.5 °C for 6 min for bead capture with iTru adaptors and primers (Glenn et al., 2016). Libraries were sent to GGBC for sequencing on a NextSeq paired-end 150bp run.

Quality of the RNASeq reads was evaluated using FastQC v.0.11.7 (http://www.bioinformatics.babraham.ac.uk/projects/fastqc/). Adapter removal and quality trimming were performed using fastp v.0.19.3 (Chen et al., 2018) using default settings. The "Tuxedo protocol", with TopHat v.2.1.1 and Cufflinks v.2.2.1, was used for the assembly of the transcriptome and differential expression analysis (Trapnell et al., 2014). Minimum and maximum intron lengths were set to 5 and 5000 respectively. Cuffdiff, included in Cufflinks, was used to find significant changes in transcript expression, using default parameters (including geometric normalization method). Transcript levels (fpkm: fragments per kilobase of transcript per million fragments mapped) in the Cuffdiff output were considered significantly different when the FDR adjusted P value was ≤0.05. The gff3 file produced by MAKER was included in TopHat, Cufflinks, and Cuffmerge runs, assigning the transcripts to genes annotated by MAKER. The same functional annotation of the corresponding genes was used for the assembled transcripts. Only those transcripts not assigned to a gene were functionally annotated by obtaining their longest open reading frame using the 'getorf' subcommand in Hmmer2Go 0.17.8 (Staton, 2018), setting the lower limit to 50 aa, and then using the obtained proteins for functional annotation as mentioned previously for the Maker-predicted proteins.

3. Results

3.1. Genome assembly and annotation

P. noxius isolate P919-02W.7 from Pohnpei was sequenced with a coverage of 130x and 230x for paired-end and mate-pair reads,

Table 1
Genome features of *Phellinus noxius* P919-02W.7 in comparison with two other published *P. noxius* genomes.

Features	*P. noxius* isolate[a]		
	P919-02W.7	OVT-YTM/97	FFPRI411160
Genome size (bp)	33,920,324	31,259,288	31,604,458
Contigs	2954	1434	16
N50	69,705	78,615	2,646,273
L50	137	122	5
Genome GC Content (%)	41.28	41.60	41.57
Predicted Genes	9389	8697	8484
Predicted Protein Coding Genes	9205	8543	8484
InterPro (Pfam) Signature	5627	5188	5169
GO Assignment (from InterProScan)	3652	3368	3352
Repetitive Elements (%)	11.74	11.49	13.38
Retroelements (%)	4.86	4.22	4.34
Transposons (%)	0.64	0.50	0.29

[a] *Phellinus noxius* isolates: P919-02W.7 (from Pohnpei, Federated States of Micronesia), OVT-YTM/97 (from Hong Kong, China), and FFPRI411160 (from Kagoshima, Kikai, Japan).

Table 2
Average nucleotide identity of *Phellinus noxius* P919-02W.7 compared to two other published *P. noxius* genomes.

Genome	OVT-YTM/97	FFPRI411160
P919-02W.7[a]	99.81/94.88/93.29[b]	99.91/95.69/93.62
FFPRI411160	99.91/95.46/93.63	

[a] *P. noxius* isolates are described in Table 1.
[b] TETRA/ANIb/ANIm methods.

respectively. The 33.92 Mbp genome assembly consisted of 2954 contigs, where the largest contig recorded was 341,158 bp. The genome features of the three *P. noxius* isolates (Pohnpei, Hong Kong, and Japan) are presented in Table 1. More than 98 % of the predicted genes in each genome assembly were predicted as protein-coding genes; of these, more than 60 % had at least one InterPro (Pfam) signature. Percent of repetitive elements was slightly higher in the isolate from Japan (FFPRI411160), and retrotransposons were more common than DNA transposons in the genomes of all three isolates.

Comparisons of the *P. noxius* genome assemblies found >99 % average nucleotide identity with the TETRA and >93 % with the ANIm methods in Pyani (Table 2). The number of predicted enzymes putatively related to pathogenicity and/or plant cell wall-degrading capacity, including proteases, carbohydrate-degrading enzymes, and lignin-degrading enzymes, were also compared across the three genomes (Table 3a). Table 3b highlights genes grouped by substrates degraded. In general, the Pohnpei isolate (P919-02W.7) had equal or slightly greater numbers across most gene families. The largest difference in the Pohnpei isolate was observed in the cytochrome P450 enzymes and proteases (Table 3a). The isolate from Japan had a larger number of glycosyl transferases, compared to the other two genomes. However, the number of AA enzymes was similar across the three genomes (Table 3b), though the total number of AA enzymes was greater in the Pohnpei isolate (Table 3a).

Genes encoding secreted proteins were notably more abundant in the genome of the Pohnpei isolate (P919-02W.7) at 562, whereas 497 and 518 were found in isolates from Hong Kong (OVT-YTM/97) and Japan (FFPRI411160), respectively (Table 4). The Pohnpei isolate also encoded a larger number of small secreted proteins (≤300 amino acids) and secreted plant cell wall carbohydrate-degrading enzymes. The Japanese isolate encoded the largest number of proteases (64) compared to Hong Kong (54) and Pohnpei (61). Interestingly, 114, 103, and 102 of cytochrome P450 enzymes were annotated in genomes of isolates from Pohnpei, Hong Kong, and Japan, respectively (Table 3): however, very few were predicted to be secreted (1, 3, and 3, respectively) (Table 4).

The number of secondary metabolite gene clusters were also compared among the three *P. noxius* genomes. Numbers were small in each of the genomes − 1 polyketide and 1 non-ribosomal synthesis clusters for each genome, ≤4 terpene synthesis clusters (3 for Pohnpei and Hong Kong and 4 for Japan) (Table 5).

3.2. Additional genome annotations of the Pohnpei isolate (P919-02W.7) using the predicted proteome

Out of the 9205 predicted proteins in the Pohnpei isolate genome, 3652 (39.6 %) had a GO term assigned during the InterProScan analyses. A considerably larger number of GO annotations were obtained using Argot 2.5 (7631; 82.9 %). Of the Biological Processes categories, oxidation-reduction process, metabolic process, and transmembrane transport had the highest representation (Fig. 1A). For Molecular Function categories, more genes grouped into hydrolase activity, ATP binding, and transferase and oxidoreductase activity (Fig. 1C). Lastly, for the Cellular Compartment categories, membrane, integral component of membrane, and nucleus were the most represented (Fig. 1E).

Using BLASTP, with the predicted proteome of Pohnpei isolate, 1537 proteins had a match (evalue ≤ 0.001) to fungal protein accessions that showed reduced virulence or loss of pathogenicity when experimentally tested or were considered effectors/plant

Table 3
Comparison of plant cell wall degrading-related proteins through annotation across three *Phellinus noxius* genome assemblies.

Enzyme	*P. noxius* isolates[a]		
	P919-02W.7	OVT-YTM/97	FFPRI411160
a. Total number of annotated			
Proteases (from InterPro)	115	107	107
Proteases (from MEROPS)	607	541	534
Carbohydrate and lignin active proteins	488	452	462
Glycosyl Transferase GT	68	67	77
Glycoside Hydrolase GH	169	157	160
Carbohydrate Binding Module CBM	36	28	29
Auxiliary Activity AA	74	70	66
Carbohydrate Esterase CE	44	43	40
Polysaccharide Lyase PL	11	10	11
Others[b]	3	3	2
Cytochrome P450	114	103	102
b. Enzymes involved in carbohydrate and lignin degradation			
Cellulose-degrading enzymes	100	92	89
Hemicellulose-degrading enzymes	97	93	92
Pectin-degrading enzymes	95	90	90
Lignin and lignin derivative-degrading enzymes	159	144	142
Laccase AA1	11	10	9
Peroxidase AA2[c]	15	15	15
Cellobiose dehydrogenase AA3	14	11	12
Vanillyl alcohol oxidase AA4	1	1	0
Glyoxal oxidase AA5	4	4	4
Cytochrome P450	114	103	102

[a] *P. noxius* isolates are described in Table 1.
[b] Lytic polysaccharide monooxygenase, cellulose-degrading enzyme (not assigned to a specific AA family); tanase-feruloyl esterase.
[c] 13 genes were confirmed by InterProScan as fungal ligninase IPR024589 domain: Fungal ligninase, C-terminal. Two had no InterPro domain hit.

Table 4
Predicted secreted proteins, proteases, and plant cell wall (PCW) carbohydrate- and lignin-degrading enzymes annotated in *Phellinus noxius* genome assemblies.

Enzyme	*P. noxius* isolates[a]		
	P919-02W.7	OVT-YTM/97	FFPRI411160
Total secreted proteins	562	497	518
Small secreted proteins	319	274	273
Proteases	61	54	64
PCW carbohydrate-degrading enzymes	112	102	106
Cellulose degrading	52	44	45
Hemicellulose degrading	31	35	32
Pectin degrading	38	34	38
Lignin and lignin derivative-degrading enzymes	30	26	28
AA1 Laccases	8	7	7
AA2 Peroxidases	13	9	12
AA3	5	5	4
AA4	0	0	0
AA5	3	2	2
Cytochrome P450	1	3	3

[a] *P. noxius* isolates are described in Table 1.

Table 5
Secondary metabolite gene clusters predicted in *Phellinus noxius* genome assemblies.

Secondary metabolite gene clusters	*P. noxius* isolates[a]		
	P919-02W.7	OVT-YTM/97	FFPRI411160
Polyketide synthesis	1	1[b]	1
Non-ribosomal synthesis	1	1[b]	1
Terpene synthesis	3	3	4

[a] *P. noxius* isolates are described in Table 1.
[b] AntiSMASH did not detect polyketide synthesis (PKS) nor non-ribosomal synthesis (NRPS) cluster. One NRPS and one type I PKS cluster were identified using a manual BLASTn search with 97 % similarity to the corresponding regions in P919-02W.7.

avirulence determinants (Supplementary Table 1) in the PHI-base, a database that includes verified pathogenicity and effector genes from fungi, bacteria, and Oomycetes. Of these, 102 were predicted as extracellular. These predicted extracellular proteins corresponded to CAZymes, peptidases, and lipases, but some also corresponded to cerato-platanin and six proteins had no annotation (Table 6). Transcripts encoding the corresponding proteins were identified for 99 of the 102 mentioned predicted extracellular proteins. Only three predicted proteins had no expression support in our analysis: one GH16, one cerato-platanin, and one WD domain G-beta repeat protein (included in the "others" category) (Table 6).

3.3. *Transcriptome analysis of* P. noxius *isolate (P919-02W.7) from Pohnpei*

Expression support in the assembled transcriptome was identified for 8806 (95.66 %) out of the total 9205 protein-coding genes. The remaining 399 (4.34 %) predicted protein-coding genes had no expression support. However, an additional 625 "novel transcripts" were assembled by the RNAseq analysis pipeline that increased the total transcripts to 9431.

Fifteen GO terms with the higher representation in *P. noxius* isolate P919-02W.7 (Pohnpei) genome are shown in a. for Biological Process, c. for Molecular Function, and e. for Cellular Compartment. Figures b, d and f, show the corresponding graphs for *P. noxius* isolate P919-02W.7 transcriptome. The 15 GO terms with the higher representation of expressed transcripts (combining the four wood substrates) were obtained (Fig. 1B, D, and F) to compare against the top 15 GO terms in the genome (Fig. 1A, C, and E). The GO profiles of expressed transcripts differed considerably from those of the genome (Fig. 1A, C, and E); categories related to protein synthesis became important in Biological Process; however, carbohydrate metabolic process remained among the top five, and pathogenesis was among the top 15. For Molecular Function categories, hydrolase activity, hydrolyzing O-glycosyl compounds, carbohydrate binding, and monooxygenase activity were among the top 15 categories of the expressed transcripts, but they were not among the top 15 in the genome. For the Cellular Component category of the expressed transcripts, membrane proteins and extracellular proteins were among the top 15 as well as fungal type cell wall. The number of transcripts in the 15 most represented GO terms in the Biological Process and Molecular Function categories, was significantly larger (adjusted $P < 2.2E\text{-}16$) for each compared to the number of genes with the same GO terms. In the Cellular Component category, only two terms had counts not significantly higher when comparing the number of transcripts versus genes ("nucleus", $P = 0.204$: and "cytosol", $P = 0.337$).

Most of the transcripts expressed by *P. noxius* isolate P919-02W.7 (Pohnpei), were similar among its growth on four different wood substrates. Although expression level of only a few transcripts differed significantly (FDR adjusted $P \leq 0.05$) among the four substrates, some transcripts were exclusive to a single substrate (Fig. 2). Of the total 114 "*Acer*-exclusive" transcripts, two had significantly higher levels of expression compared to the other three wood substrates, but no annotation was found for either transcript. The remaining 112 were present but did not have expression values significantly different from zero, likely because the variance observed in the two replicates. No transcripts in the "*Pinus*-exclusive", "*Prunus*-exclusive", and "*Salix*-exclusive" sets showed such significance. However, a few more transcripts were found with statistically significant different levels of expression when all transcripts were compared. Transcripts produced on the *Acer* substrate showed the most differences with 18 transcripts expressed at significantly higher levels: five in comparison to *Pinus* substrate, nine in comparison to *Prunus* substrate, and four in

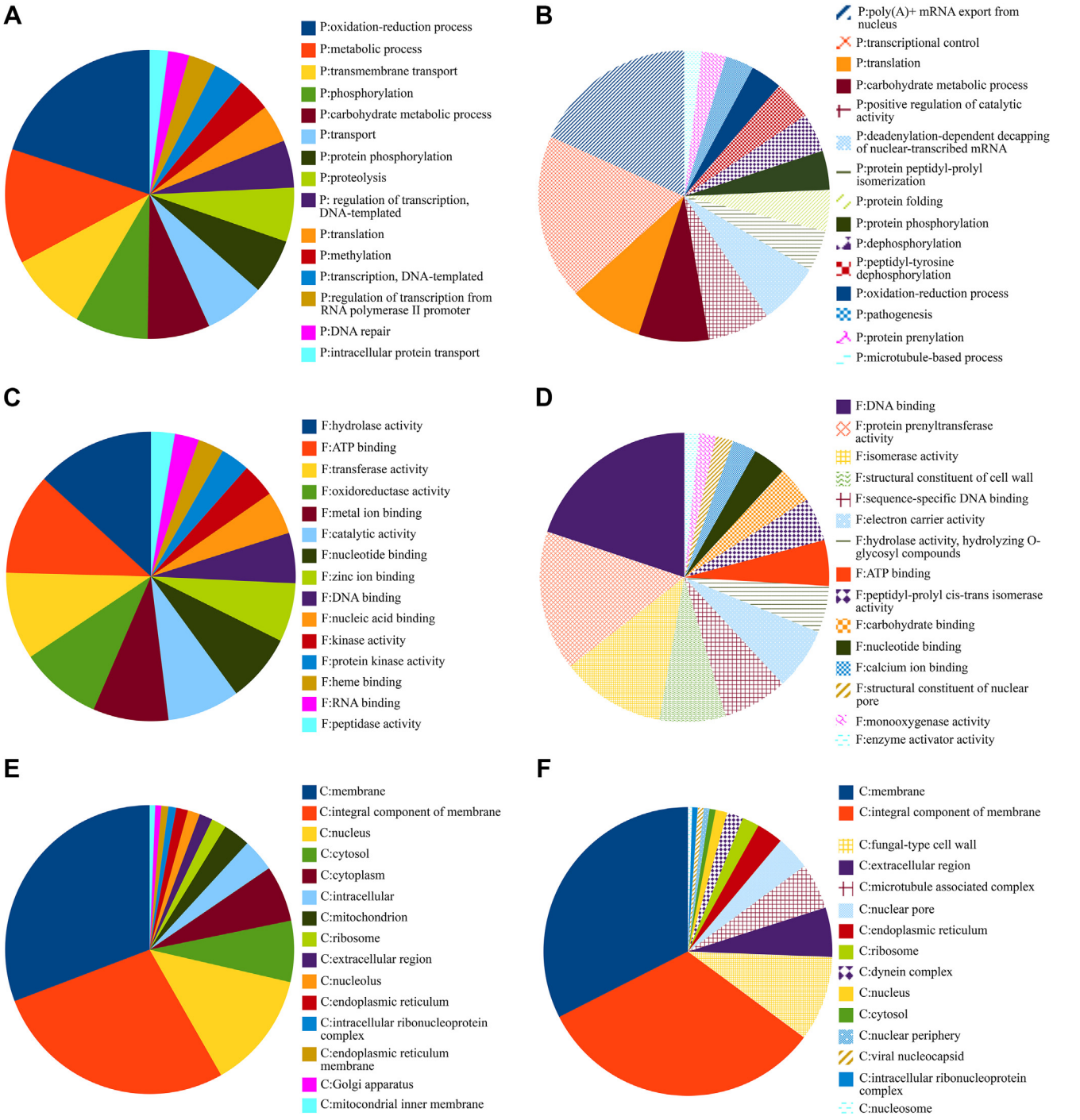

Fig. 1. Fifteen GO terms with the higher representation in *Phellinus noxius* isolate P919-02W.7 (Pohnpei) genome are shown in A. for Biological Process, C. for Molecular Function, and E. for Cellular Compartment. Figures B, D and F, show the corresponding graphs for *P. noxius* isolate P919-02W.7 transcriptome.

comparison to *Salix* substrate. On the *Prunus* substrate, 16 transcripts displayed significantly higher expression transcripts: seven in comparison to *Acer*, six in comparison to *Pinus*, and three in comparison to *Salix*. The *Salix* substrate resulted in nine transcripts with a significantly higher expression level: four when compared to *Acer* substrate, four when compared to *Pinus* substrate, and one when compared to *Prunus* substrate. Finally, *Pinus* had seven transcripts with significantly higher expression levels: one, five, and one in comparison to *Acer, Prunus*, and *Salix* substrates, respectively (Supplementary Table 2). Transcripts coding for thaumatin, cysteine-rich protein, fungal hydrophobin, and fungal ligninase (AA2) were among those with significantly higher expression that were also predicted to be secreted. The other transcripts had little or no annotation (Supplementary Table 2).

Expression levels of transcripts corresponding to predicted secreted, plant cell wall carbohydrate- and lignin-degrading enzymes, and secreted proteases were obtained for *P. noxius* isolate P919-02W.7 (Pohnpei) growing on each wood substrate. Then, transcript levels for each class were grouped together (Fig. 3), and grouped by their functional substrate (Fig. 4). Both figures highlight

Table 6
Annotation of *Phellinus noxius* isolate P919-02W.7 (Pohnpei) predicted secreted proteins with PHI-base match to reduced or loss of virulence, or identified as effectors.

Protein	Substrate/function	Number
AA1	Cellulose/Lignin	4
AA2	Lignin	13
AA3	Cellulose/Lignin	5
AA5	Lignin	3
AA8	Cellulose	1
AA9	Cellulose	2
CBM	Carbohydrate binding	9
CE16	Hemicellulose	1
GH10	Hemicellulose	3
GH12	Cellulose	1
GH125	Mannose	1
GH13	Starch	1
GH15	Starch	1
GH16	Pectin	4
GH18	Chitin	2
GH20	Acetyl/galactyl glucosamide	1
GH28	Pectin	1
GH3	Cellulose/Pectin	1
GH31	Hemicellulose/Pectin	1
GH5	Cellulose/Hemicellulose/Pectin	7
GT90	Carbohydrate synthesis	1
PL1	Pectin	3
Peptidase	Proteins	13
Lipase	Lipids	6
Amidase	Amides	1
Cerato-platanin	Cell wall loosening	4
Cysteine-rich secretory protein family	Not clear function	3
LysM domain protein	Chitin binding	2
Other	Multiple substrates	13
no annotation		6

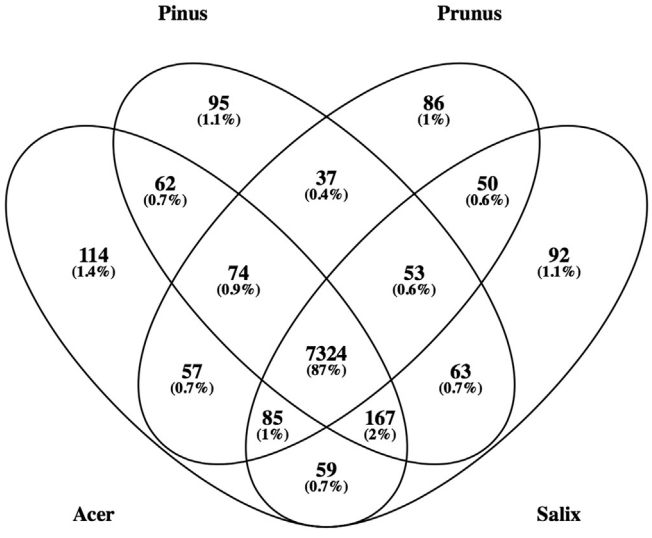

Fig. 2. This shows exclusive and shared transcripts for *Phellinus noxius* isolate P919-02W.7 (Pohnpei) on four wood substrates. Although approximately 1 % of the transcripts was exclusive for each wood substrate, few differences were found in transcript annotations. Levels of expression were not significantly different for wood substrates, *Pinus*, *Prunus*, *Salix*, and for *Acer* only 2/144 were differentially expressed.

the similarities among expressed transcripts for each wood type though slight differences exist.

4. Discussion

This current study increases our understanding of wood-degrading mechanisms of *P. noxius*. Genomics and transcriptomics were used to explore the repertoire of *P. noxius* genes encoding plant cell wall-degrading enzymes in the genome and gene expression in association with colonization of different wood substrates (*Acer*, *Prunus*, *Salix*, and *Pinus*). Compared with other white-rot fungi, *P. noxius* possesses a relatively similar range and variety of genes for degrading cellulose, hemicellulose, lignin, and pectin (Rytioja et al., 2014; Nagy et al., 2016). In addition, this pathogen expressed relatively similar genes across four wood substrates derived from one gymnosperm (*Pinus*) and three angiosperms (*Acer*, *Prunus*, and *Salix*) at this saprophytic stage (6 weeks post inoculation), though the proportions of cellulose, hemicellulose, lignin, and pectin vary among the substrates (Serapiglia et al., 2008; Emandi et al., 2011).

The genome sizes of *P. noxius* isolates from Pohnpei, Hong Kong, and Japan ranged from 31.60 to 33.92 Mb, which is relatively smaller compared with other Basidiomycota fungi that are reported to have an average genome size of 46.48 Mb (Mohanta and Bae, 2015). Percent of repetitive elements comprised a slightly higher proportion (13.38 %) of the genome for the isolate from Japan, but the range of repetitive elements in the genomes of the three isolates was at an intermediate level compared to most sequenced fungi (3–20 %) (Santana and Queiroz, 2015). Retrotransposons accounted for a higher proportion of the genome than DNA transposons, a feature commonly observed in fungal genomes (Muszewska et al., 2017).

The genetic similarities among genomes of the three *P. noxius* isolates from Asia–Pacific regions were around 99 %, 95 %, and 93 % using TETRA, ANIb, and ANIm methodologies, respectively, with only slight variations in genome features. Chung et al. (2017) highlighted an average of 97 % genetic differences among isolates from Hong Kong compared to isolates belonging to a well-described *P. noxius* lineage from Taiwan and the Ryuku Islands of Japan (Sahashi et al., 2014; Stewart et al., In press). For the present study, the isolate from Japan was identified by Chung et al. (2017) as

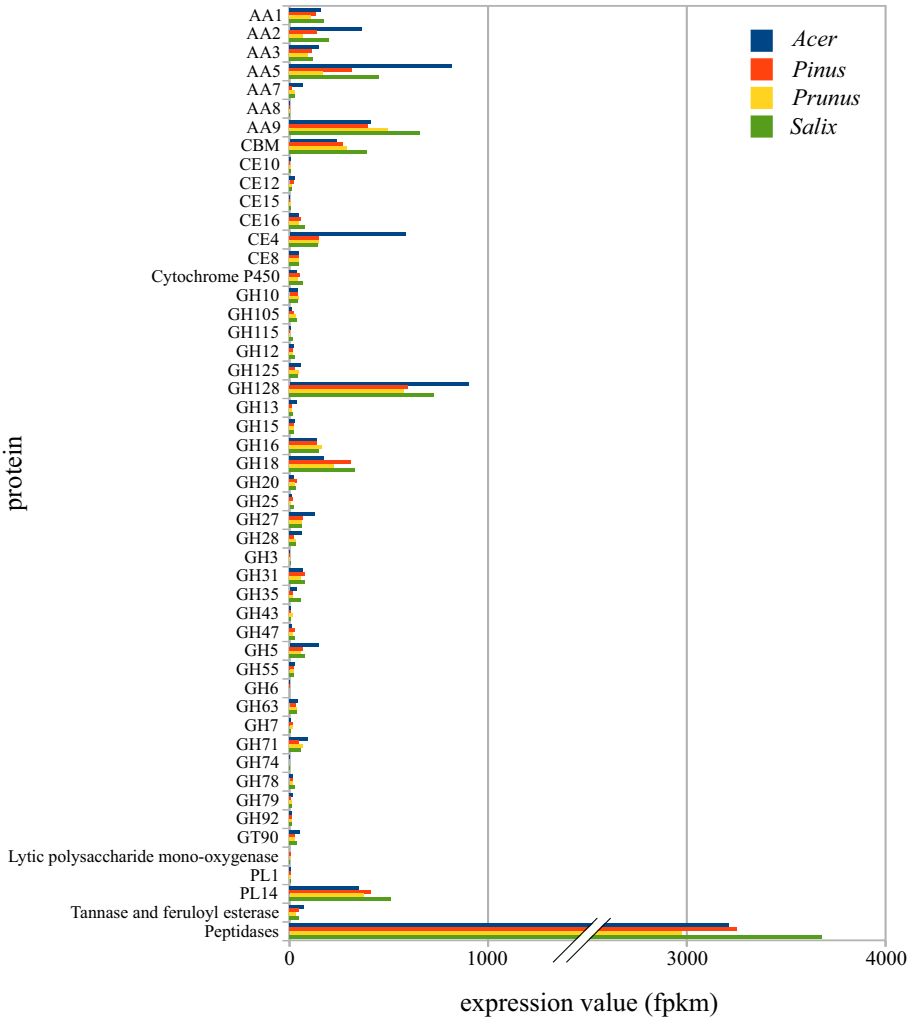

Fig. 3. Levels of expression of transcripts encoding predicted secreted, plant cell wall (PCW) degrading enzymes and peptidases of *Phellinus noxius* isolate P919-02W.7 (Pohnpei) on four wood substrates (*Pinus*, *Prunus*, *Salix*, and *Acer*).

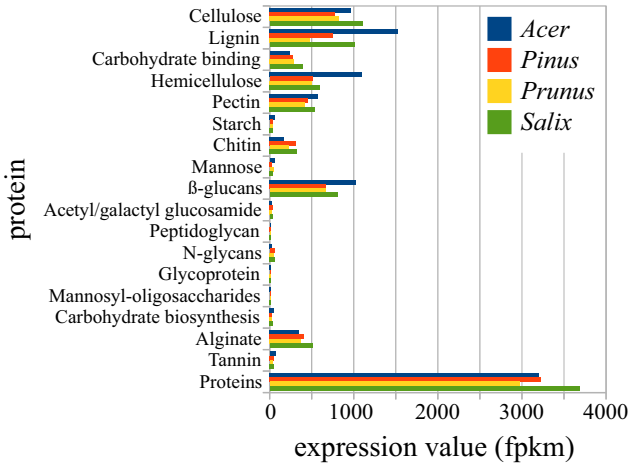

Fig. 4. Levels of expression of transcripts encoding predicted secreted, plant cell wall (PCW) degrading enzymes and peptidases of *Phellinus noxius* isolate P919-02W.7 on four wood substrates (*Pinus*, *Prunus*, *Salix*, and *Acer*) grouped by their corresponding substrate.

part of the Taiwan/Ryuku lineage. When examining nucleotide differences among the isolates, averaged across the three methods, we find that the Pohnpei and Japan isolates are slightly more similar at 96.41 %, than the Pohnpei and Hong Kong isolates at 95.99 %. Though the differences are slight, these results concur with other reports suggesting that isolates from Ryuku Islands of Japan and isolates from islands of the South Pacific (Stewart et al., In press) provide potential insights into the migration and gene flow of *P. noxius* among eastern Asian islands and other Pacific Islands.

Genome-based analyses have shown that CAZymes vary significantly across wood-degrading Basidiomycota, especially between white-rot fungi, which degrade lignin and cellulose, and brown-rot fungi, which degrade cellulose (Nagy et al., 2016). A larger number of lignin-degrading enzymes, including laccases, peroxidases, and cytochrome P450 monooxygenases, have been observed in the genomes of white-rot fungi compared to those of brown-rot and soft-rot fungi, which likely explains the efficiency and suitability of white-rot fungi to degrade lignin (Kameshwar and Qin, 2018; Rytioja et al., 2014). The *P. noxius* genome and transcriptomic analyses highlighted a vast portfolio of predicted secreted, lignin-degrading enzymes, such as laccases (AA1 genes;

ca. 9–11) and lignin peroxidases (AA2 genes; ca. 15). In our annotation of *P. noxius* genes, 13 of genes were confirmed by InterProScan as fungal ligninase IPR024589 domain: fungal ligninase, C-terminal; however, two of the identified AA2 genes had no InterPro domain hit (identification). This is consistent with another white-rot fungus, *Pycnoporus cinnabarinus*, for which its genome was found to encode five laccases and nine AA2 peroxidases (Levasseur et al., 2014). Abundance of the AA2 genes was suggested by Riley et al. (2014) and Floudas et al. (2012) to be the main consideration for the classification of a wood-rot fungi as a white-rotter, because the AA2 gene family is absent in all brown-rot fungi examined thus far.

Cytochrome P450 genes were also abundant, ranging from 102 to 114 in the three genomes, which may provide some evidence for the broad host range of *P. noxius*. Functional analyses of cytochrome P450s in fungi have shown their catalytic versatility in modifying metabolic systems, allowing a species to thrive in and adapt to diverse physiological and/or biodegradation conditions (Črešnar and Petrič, 2011; Subramanian and Yadav, 2008; Shin et al., 2018; Syed and Yadav, 2012). Further, enrichment of cytochrome P450s enzymes has also been linked to wood colonization, for example *Armillaria mellea*, a hardwood rot pathogen has been documented to have 267 cytochrome P450s, whereas rust fungi have been shown to only have approximately 20 cytochrome P450s (Qhanya et al., 2015). Aside from lignin degradation, enzymes for cellulose degradation [glycoside hydrolases appended to carbohydrate-binding modules (CBMs)] were also abundant in *P. noxius*, another common characteristic among white-rot fungi (Riley et al., 2014).

Abundance of genes in the genome does not necessarily correspond to the abundance of transcripts; however, most of the available genes were transcribed by *P. noxius* isolate P919-02W.7 (Pohnpei) during colonization of the four wood substrates examined, including *Pinus, Prunus, Salix*, and *Acer*, but corresponding transcripts were produced at different levels. Especially interesting is the presence of the GO term "carbohydrate metabolic process" among the top 15 in the Biological Process category in both the genome and transcriptome of *P. noxius.* Also noteworthy is the presence of "pathogenesis" among the top 15 in Biological Process in the transcriptome, as well as "hydrolase activity, hydrolyzing O-glycosyl compounds", "carbohydrate binding," and "monooxygenase activity" in the Molecular Function category. Abundance of CAZyme-encoding transcripts provided more evidence that *P. noxius* is capable of lignocellulosic catabolism. With all substrates, CAZyme families, including the white-rot exclusive AA2, other laccase genes families, and peroxidase genes families were expressed during saprophytic colonization of the wood substrates. Similarly, the saprophytic white-rot fungus, *Pycnoporus coccineus*, transcribed CAZyme-encoding genes at high levels when subjected to lignocellulosic material (Miyauchi et al., 2017). Likewise, a majority of CAZyme transcripts, such as peroxidases, were upregulated in *Phlebia radiata* during cell-wall degradation of spruce wood (Kuuskeri et al., 2016).

Insights on fungal responses during colonization of different wood substrates can help identify pathogenicity mechanisms for various known and potential hosts. The tree species used as substrates in this study were selected to generally represent diverse structural chemistry found in wood associated with a broad host range. We expected that gene expression would vary significantly between the broadleaved/angiosperm substrates (*Acer*, *Prunus* and *Salix*) compared to the coniferous/gymnosperm substrate (*Pinus*), because of the differences in cellulose and lignin content. However, after 6 weeks, only slight differences in gene expression were observed across wood substrates, and about 87 % of the transcripts were shared among the *Acer*, *Pinus*, *Prunus*, and *Salix* substrates. Similar gene expression across diverse wood substrates could be attributable to several factors. Our experiment included only two replicates for each wood substrate, and the high variance in expression levels between the two replicates limited the detection of significant differences in expressed transcripts among wood substrates. Further, sterilization by autoclaving may have altered the cell wall composition of the wood substrates in a manner that influenced gene expression by *P. noxius*, and/or differences in gene expression could perhaps occur before or after the 6-week incubation period. Similar results were found in the transcriptome analysis of *Phanerochaete chrysosporium*, while variation in gene expression of the differentially regulated genes was linked to wood substrates at 10 and 20 d, no significant substrate-dependent gene expression was observed after the 30 d incubation (Skyba et al., 2016). Another study found that gene expression of *Phlebia radiata* on spruce wood changed over time as sugar became more available after lignin degradation (Kuuskeri et al., 2016). Therefore, we postulate that the composition of different wood substrates may have become more similar after 6-weeks incubation. Another possibility is that entire suites of genes that encode cell-wall degrading enzymes could be upregulated in unison, regardless of substrate type. Unfortunately, our data could not distinguish between these hypotheses, because additional time points during colonization and degradation were unavailable.

Given the vast suite of cell wall-degrading enzymes of *P. noxius*, it is likely that the pathogen can decompose host species outside its known host range, at least during its saprophytic stage. This study presents the genome and transcriptome of *P. noxius* isolate from Pohnpei (Federated States of Micronesia), which was collected >4000 km from the *P. noxius* isolates from Japan and Hong Kong, China. Further comparisons across the *P. noxius* lineages may elucidate differences in host range, virulence, or environmental requirements. Evolutionary histories of Agaricomycete white-rot fungi suggest a transition between degrading diverse host species (host generalist) toward more focused host species (host specialist) in angiosperms (Krah et al., 2018). Although a number of species within the Hymenochaetales have been classified as angiosperm specialists (Krah et al., 2018), *P. noxius* has the capacity to degrade wood of species within both gymnosperms and angiosperms, which may suggest a generalist lifestyle. Sahashi et al. (2014) demonstrated the possibility of pathogen invasion by *P. noxius,* as this species was able to effectively infect four commercially and ecologically important temperate conifer species including *Chamaecyparis obtusa, Cryptomeria japonica, Larix kaempferi*, and *Pinus thunbergii*. Thus, this current study provides additional molecular evidence of potential invasive risk of *P. noxius* to degrade the substrates of various woody species. Further studies on global movement of *P. noxius* across temperate and tropical regions would be greatly relevant, as climate change progresses to potentially promote a more conducive environment for the pathogen in new geographic areas. Further, molecular research may improve our understanding on pathogenicity and decomposition capacities across populations and lineages of *P. noxius*.

Acknowledgements

This research was supported by USDA – Forest Service (FS), Forest Health Protection – Special Technology Development Program (STDP-R5-2015-1 and STDP-R5-2019-2), USDA – FS, Rocky Mountain Research Station and Pacific Northwest Research Station, Research Joint Venture Agreement (15-JV-11221633-160 and 19-JV-11221633-093 to JES, and 14-JV-11221633-117 to Western Forestry and Conservation Association) and the National Science Foundation (grant DEB-1136626 to TCG). The authors thank Yuko Ota and Norio Sahashi for *P. noxius* isolation, Sara Ashiglar for establishing the

wood substrate study, Brant Faircloth and the Georgia Genomics and Bioinformatics Core staff for assistance with genomics and transcriptomics.

Appendix A. Supplementary data

Supplementary data to this article can be found online at https://doi.org/10.1016/j.funbio.2019.12.007.

References

Akiba, M., Ota, Y., Tsai, I.J., Hattori, T., Sahashi, N., Kikuchi, T., 2015. Genetic differentiation and spatial structure of *Phellinus noxius*, the causal agent of brown root rot of woody plants in Japan. PLoS One 10, e0141792. https://doi.org/10.1371/journal.pone.0141792.

Almagro Armenteros, J.J., Kaae Sønderby, C., Kaae Sønderby, S., Nielsen, H., Winther, O., 2017. DeepLoc: prediction of protein subcellular localization using deep lerning. Bioinformatics 33, 3387–3395.

Ann, P.-J., Lee, H.-L., Huang, T.-C., 1999. Brown root rot of 10 species of fruit trees caused by *Phellinus noxius* in Taiwan. Plant Dis. 83, 746–750.

Ann, P.-J., Chang, T.-T., Ko, W.-H., 2002. *Phellinus noxius* brown root rot of fruit and ornamental trees in Taiwan. Plant Dis. 86, 820–826.

Bergeron, M.-J., Feau, N., Stewart, D., Tanguay, P., Hamelin, R.C., 2019. Genome-enhanced detection and identification of fungal pathogens responsible for pine and poplar rust diseases. PLoS One 14, e0210952. https://doi.org/10.1371/journal.pone.0210952.

Blin, K., Wolf, T., Chevrette, M.G., Lu, X., Schwalen, C.J., Kautsar, S.A., Suarez Duran, H.G., de Los Santos, E.L.C., Kim, H.U., Nave, M., Dickschat, J.S., Mitchell, D.A., Shelest, E., Breitling, R., Takano, E., Lee, S.Y., Weber, T., Medema, M.H., 2017. antiSMASH 4.0-improvements in chemistry prediction and gene cluster boundary identification. Nucleic Acids Res. 45 (W1), W36–W41. https://doi.org/10.1093/nar/gkx319.

Bolland, L., 1984. *Phellinus noxius*: cause of a significant root-rot in Queensland hoop pine plantations. Aust. For. 47, 2–10.

Brooks, F., 2002. Brown root rot disease in American Samoa's tropical rain forests. Pac. Sci. 56, 377–387.

CABI, 2018. *Phellinus noxius* (brown tea root disease). Invasive Species Compendium. CAB International, Wallingford, UK. https://www.cabi.org/isc/datasheet/40154.

Camacho, C., Coulouris, G., Avagyan, V., Ma, N., Papadopoulos, J., Bealer, K., Madden, T.L., 2009. BLAST+: architecture and applications. BMC Bioinf. 10, 421–429.

Cantarel, B.L., Korf, I., Robb, S.M.C., Parra, G., Ross, E., Moore, B., Holt, C., Sánchez Alvarado, A., Yandell, M., 2008. MAKER: an easy-to-use annotation pipeline designed for emerging model organism genomes. Genome Res. 18, 188–196.

Chang, T.T., 1996. Survival of *Phellinus noxius* in soil and in the roots of dead host plants. Phytopathology 86, 272–276.

Chen, S., Zhou, Y., Chen, Y., Gu, J., 2018. fastp: an ultra-fast all-in-one FASTQ preprocessor. Bioinformatics 34, i884–i890.

Chung, C.-L., Huang, S.-Y., Huang, Y.-C., Tzean, S.-S., Ann, P.-J., Tsai, J.-N., Yang, C.-C., Lee, H.-H., Huang, T.-W., Huang, H.-Y., Chang, T.-T., Lee, H.-L., Liou, R.-F., 2015. The genetic structure of *Phellinus noxius* and dissemination pattern of brown root rot disease in Taiwan. PLoS One 10 (10), e0139445. https://doi.org/10.1371/journal.pone.0139445.

Chung, C.-L., Lee, T.J., Akiba, M., Lee, H.-H., Kuo, T.-H., Liu, D., Ke, H.-M., Yokoi, T., Roa, M.B., Lu, M.-Y., Chang, Y.-Y., Ann, P.-J., Tsai, J.-N., Chen, C.-Y., Tzean, S.-S., Ota, Y., Hattori, T., Sahashi, N., Liou, R.-F., Kikuchi, T., Tsai, I.J., 2017. Comparative and population genomic landscape of *Phellinus noxius:* a hypervariable fungus causing root rot in trees. Mol. Ecol. 26, 6301–6316. https://doi.org/10.1111/mec.14359.

Črešnar, B., Petrič, Š., 2011. Cytochrome P450 enzymes in the fungal kingdom. Biochim. Biophys. Acta 1814, 29–35.

Emandi, A., Vasiliu, C.I., Budrugeac, P., Stamatin, I., 2011. Quantitative investigation of wood composition by integrated FT-IR and thermogravimetric methods. Cellul. Chem. Technol. 45, 579–584.

Feau, N., Beauseigle, S., Bergeron, M., Bilodeau, G.J., Birol, I., Cervantes-Arango, S., Dhillon, B., Dale, A.L., Herath, P., Jones, S.J.M., Lamarche, J., Ojeda, D.I., Sakalidis, M.L., Taylor, G., Tsui, C.K.M., Uzunovic, A., Yueh, H., Tanguay, P., Hamelin, R.C., 2018. Genome-enhanced detection and identification (GEDI) of plant pathogens. Peer J. 6, e4392 https://doi.org/10.7717/peerj.4392.

Floudas, D., Binder, M., Riley, R., Barry, K., Blanchette, R.A., Henrissat, B., Martinez, A.T., Otillar, R., Spatafora, J.W., Yadav, J.S., Aerts, A., Benoit, I., Boyd, A., Carlson, A., Copeland, A., Coutinho, P.M., de Vries, R.P., Ferreira, P., Findley, K., Foster, B., Gaskell, J., Glotzer, D., Gorecki, P., Heitman, J., Hesse, C., Hori, C., Igarashi, K., Jurgens, J.A., Kallen, N., Kersten, P., Kohler, A., Kues, U., Arun Kumar, T.K., Kuo, A., LaButti, K., Larrondo, L.F., Lindquist, E., Ling, A., Lombard, V., Lucas, S., Lundell, T., Martin, R., McLaughlin, D.J., Morgenstern, I., Morin, E., Murat, C., Nagy, L.G., Nolan, M., Ohm, R.A., Patyshakuliyeva, A., Rokas, A., Ruiz-Dueñas, F.J., Sabat, G., Salamov, A., Samejima, M., Schmutz, J., Slot, J.C., St. John, F., Stenlid, J., Sun, H., Sun, S., Syed, K., Tsang, A., Wiebenga, A., Young, D., Pisabarro, A., Eastwood, D.C., Martin, F., Cullen, D., Grigoriev, I.V., Hibbett, D.S., 2012. The Paleozoic origin of enzymatic lignin decomposition reconstructed from 31 fungal genomes. Science 336, 1715–1719. https://doi.org/10.1126/science.1221748.

Floudas, D., Held, B.W., Riley, R., Nagy, L.G., Koehler, G., Ransdell, A.S., Younus, H., Chow, J., Chiniquy, J., Lipzen, A., Tritt, A., Sun, H., Haridas, S., LaButti, K., Ohm, R.A., Kües, U., Blanchette, R.A., Grigoriev, I.V., Minto, R.E., Hibbett, D.S., 2015. Evolution of novel wood decay mechanisms in Agaricales revealed by the genome sequences of *Fistula hepatica* and *Cylindrobasidium torrendii*. Fungal Genet. Biol. 76, 78–92.

Glenn, T.C., Nilsen, R.A., Kieran, T.J., Sanders, J.G., Bayona-Vásquez, N.J., Finger Jr., J.W., Pierson, T.W., Bentley, K.E., Hoffberg, S.L., Louha, S., García-De León, F.J., Del Río-Portilla, M.A., Reed, K.D., Anderson, J.L., Meece, J.K., Aggrey, S.E., Rekaya, R., Alabady, M., Bélanger, M., Winker, K., Faircloth, B.C., 2016. Adapterama I: universal stubs and primers for 384 unique dual-indexed or 147,456 combinatorially-indexed Illumina libraries (iTru & iNext). bioRxiv 049114. https://doi.org/10.1101/049114.

Ibarra Caballero, J.R., Jeon, J., Lee, Y.H., Fraedrich, S., Klopfenstein, N.B., Kim, M.-S., Stewart, J.E., 2019. Genomic comparisons of the laural wilt pathogen, *Raffaelea lauricola*, and related tree pathogens highlight an arsenal of pathogenicity related genome. Fungal Genet. Biol. 125, 84–92.

Ichinose, H., 2013. Cytochrome P450 of wood-rotting basidiomycetes and biotechnological applications. Biotechnol. Appl. Biochem. 60, 71–81.

Janusz, G., Pawlik, A., Sulej, J., Swiderska-Burek, U., Jarosz-Wilkolazka, A., Paszczynski, A., 2017. Lignin degradation: microorganisms, enzymes involved, genomes analysis and evolution. FEMS Microbiol. Rev. 41, 941–962.

Jones, P., Binns, D., Chang, H., Fraser, M., Li, W., McAnulla, C., McWilliam, H., Maslen, J., Mitchell, A., Nuka, G., Pesseat, S., Quinn, A.F., Sangrador-Vegas, A., Scheremetjew, M., Yong, S., Lopez, R., Hunter, S., 2014. InterProScan 5: genome-scale protein function classification. Bioinformatics 30, 1236–1240.

Kameshwar, A.K.S., Qin, W., 2018. Comparative study of genome-wide plant biomass-degrading CAZymes in white-rot, brown rot and soft rot fungi. Mycology 2, 93–105. https://doi.org/10.1080/21501203.2017.1419296.

Keller, O., Kollmar, M., Stanke, M., Waack, S., 2011. A novel hybrid gene prediction method employing protein multiple sequence alignments. Bioinformatics 27, 757–763. https://doi.org/10.1093/bioinformatics/btr010.

Kovalchuk, A., Zeng, Z., Ghimire, R.P., Kivimaenpaa, M., Raffaello, T., Liu, M., Mukrimin, M., Kasanen, R., Julkunen-Tiitto, R., Holopainen, J.K., Asiegbu, F.O., 2019. Dual RNA-seq analysis provided new insights into interactions between Norway spruce and necrotrophic pathogen *Heterobasidion annosum* s.l. BMC Plant Biol. 19, 2. https://doi.org/10.1186/s12870-018-1602-0.

Krah, F.-S., Seibold, S., Brandl, R., Baldrian, P., Müller, J., Bässler, C., 2018. Independent effects of host and environment on the biodiversity of wood-inhabiting fungi. J. Ecol. 106, 1428–1442. https://doi.org/10.1111/1365-2745.12939.

Kuuskeri, J., Häkkinen, M., Laine, P., Smolander, O.-P., Tamene, F., Miettinen, S., Nousiainen, P., Kemell, M., Auvinen, P., Lundell, T., 2016. Time-scale dynamics of proteome and transcriptome of the white-rot fungus *Phlebia radiata*: growth on spruce wood and decay effect on lignocellulose. Biotechnol. Biofuels 9, 192.

Lavezzo, E., Falda, M., Fontana, P., Bianco, L., Toppo, S., 2016. Enhancing protein function prediction with taxonomic constraints – the Argot2.5 web server. Methods 93, 15–23.

Levasseur, A., Drula, E., Lombard, V., Coutinho, P.M., Henrissat, B., 2013. Expansion of the enzymatic repertoire of the CAZy database to integrate auxiliary redox enzymes. Biotechnol. Biofuels 6, 41–55.

Levasseur, A., Lomascolo, A., Chabrol, O., Ruiz-Deuñas, F.J., Boukhris-Uzan, E., Piumi, F., Kües, U., Ram, A.F.J., Murat, C., Haon, M., Benoit, I., Arfi, Y., Chevret, D., Drula, E., Kwon, M.J., Gouret, P., Lesage-Meessen, L., Lombard, V., Mariette, J., Noirot, C., Park, J., Patyshakuliyeva, A., Sigoillot, J.C., Wiebenga, A., Wösten, H.A.B., Martin, F., Coutinho, P.M., de Vries, R.P., Martínez, A.T., Klopp, C., Pontarotti, P., Henrissat, B., Record, E., 2014. The genome of the white-rot fungus *Pycnoporus cinnabarinus*: a basidiomycete model with a versatile arsenal for lignocellulosic biomass breakdown. BMC Genomics 15, 486.

Levasseur, A., Piumi, F., Coutinho, P.M., Rancurel, C., Asther, M., Delattre, M., Henrissat, B., Pontarotti, P., Asther, M., Record, E., 2008. FOLy: an integrated database for the classification and functional annotation of fungal oxidoreductases potentially involved in the degradation of lignin and related aromatic compounds. Fungal Genet. Biol. 45, 638–645. https://doi.org/10.1016/j.fgb.2008.01.004.

Lombard, V., Golaconda Ramulu, H., Drula, E., Coutinho, P.M., Henrissat, B., 2014. The carbohydrate-active enzymes database (CAZy) in 2013. Nucleic Acids Res. 42, D490–D495. https://doi.org/10.1093/nar/gkt1178.

Miyauchi, S., Navarro, D., Grisel, S., Chevret, D., Berrin, J.-G., Rosso, M.-N., 2017. Integrative omics of white-rot *Pycnoporus coccineus* reveals co-regulated CAZymes for orchestrated lignocellulose breakdown. PLoS One 12 (4), e0175528. https://doi.org/10.1371/journal.pone.0175528.

Mohanta, T.K., Bae, H., 2015. The diversity of fungal genome. Biol. Proc. 17, 8. https://doi.org/10.1186/s12575-015-0020-z.

Muszewska, A., Steczkiewicz, K., Stepniewska-Dziubinska, M., Ginalski, K., 2017. Cut-and-paste transposons in fungi with diverse lifestyles. Genome Biol. Evol. 9 (12), 3463–3477. https://doi.org/10.1093/gbe/evx261.

Nagy, L.G., Riley, R., Tritt, A., Adam, C., Daum, C., Floudas, D., Sun, H., Yadav, J.S., Pangilian, J., Larsson, K.-H., Matsuura, K., Barry, K., Labutti, K., Kuo, R., Ohm, R.A., Bhattacharya, S.S., Shirouzu, T., Yoshinaga, Y., Martin, F.M., Grigoriev, I.V., Hibbett, D.S., 2016. Comparative genomics of early-diverging mushroom-forming

fungi provides insights into the origins of lignocellulose decay capabilities. Mol. Biol. Evol. 33 (4), 959–970. https://doi.org/10.1093/molbev/msv337.
Ohm, R.A., Riley, R., Salamov, A., Min, B., Choi, I.G., Grigoriev, I.V., 2014. Genomics of wood-degrading fungi. Fungal Genet. Biol. 72, 82–90. https://doi.org/10.1016/j.fgb.2014.05.001.
Plissonneau, C., Benevenuto, J., Mohd-Assaad, N., Fouché, S., Hartmann, F.E., Croll, D., 2017. Using population and comparative genomics to understand the genetic basis of effector-driven fungal pathogen evolution. Front. Plant Sci. 8, 119. https://doi.org/10.3389/fpls.2017.00119.
Qhanya, L.B., Matowane, G., Chen, W., Sun, Y., Letsimo, E.M., Parvez, M., Yu, J.H., Mashele, S.S., Syed, K., 2015. Genome-wide annotation and comparative analysis of cytochrome P450 monooxygenases in basidiomycete biotrophic plant pathogens. PLoS One 10 (11), e0142100. https://doi.org/10.1371/journal.pone.0142100.
Rawlings, N.D., Barrett, A.J., Thomas, P.D., Huang, X., Bateman, A., Finn, R.D., 2018. The MEROPS database of proteolytic enzymes, their substrates and inhibitors in 2017 and a comparison with peptidases in the PANTHER database. Nucleic Acids Res. 46, D624–D632. Database issue.
Riley, R., Salamov, A.A., Brown, D.W., Nagy, L.G., Floudas, D., Held, B.W., Levasseur, A., Lombard, V., Morin, E., Otillar, R., Lindquist, E.A., Sun, H., LaButti, K.M., Schmutz, J., Jabbour, D., Luo, H., Baker, S.E., Pisabarro, A.G., Walton, J.D., Blanchette, R.A., Henrissat, B., Martin, F., Cullen, D., Hibbett, D.S., Grigoriev, I.V., 2014. Extensive sampling of basidiomycete genomes demonstrate inadequacy of the white-rot/brown-rot paradigm for wood decay fungi. PNAS 111 (27), 9923–9928. www.pnas.org/cgi/doi/10.1073/pnas.1400592111.
Ross-Davis, A.L., Stewart, J.E., Hanna, J.W., Kim, M.-S., Knaus, B.J., Cronn, R., Rai, H., Richardson, B.A., McDonald, G.I., Klopfenstein, N.B., 2013. Transcriptome of an Armillaria root disease pathogen reveals candidate genes involved in host substrate utilization at the host -pathogen interface. For. Pathol. 43, 468–477. https://doi.org/10.1111/efp.12056.
Rytioja, J., Hilden, K., Yuzon, J., Hatakka, A., de Vries, R.P., Mäkela, M.R., 2014. Plant-polysaccharide-degrading enzymes from basidiomycetes. Microbiol. Mol. Biol. Rev. 78 (4), 614–649. https://doi.org/10.1128/MMBR.00035-14.
Sahashi, N., Akiba, M., Ishihara, M., Ota, Y., Kanzaki, N., 2012. Brown root rot of trees caused by *Phellinus noxius* in the Ryukyu Islands, subtropical areas of Japan. For. Pathol. 42, 353–361. https://doi.org/10.1111/j.1439-0329.2012.00767.x.
Sahashi, N., Akiba, M., Takemoto, S., Yokoi, T., Ota, Y., Kanzaki, N., 2014. *Phellinus noxius* causes brown root rot on four important conifer species in Japan. Eur. J. Plant Pathol. 140, 869–873. https://doi.org/10.1007/s10658-014-0503-9.
Santana, M.F., Queiroz, M.V., 2015. Transposable elements in fungi: a genomic approach. Sci. J Genet. Gene. Ther. 1 (1), 12–16.
Serapiglia, M.J., Cameron, K.D., Stipanovic, A.J., Smart, L.B., 2008. High-resolution thermogravimetric analysis for rapid characterization of biomass composition and selection of shrub willow varieties. Appl. Biochem. Biotechnol. 145, 3–11. https://doi.org/10.1007/s12010-007-8061-7.
Shin, J., Kim, J.-E., Lee, Y.-W., Son, H., 2018. Fungal cytochrome P450s and the P450 complement (CYPome) of *Fusarium graminearum*. *Toxins* 10 (3), 112. https://doi.org/10.3390/toxins10030112.
Skyba, O., Cullen, D., Dougla, s C.J., Mansfield, S.D., 2016. Gene expression patterns of wood decay fungi *Postia placenta* and *Phanerochaete chrysosporium* are influenced by wood substrate composition during degradation. Appl. Environ. Microbiol. 82, 4387–4400. https://doi.org/10.1128/AEM.00134-16.
Smit, A.F.A., Hubley, R., 2017. RepeatModeler. http://repeatmasker.org.
Smit, A.F.A., Hubley, R., Green, P., 2015. RepeatMasker. http://repeatmasker.org.
Stewart, J.E., Kim, M.-S., Hanna, J.W., Ota, Y., Otto, K., Akiba, M., Atibalentia, N.,Brooks, F., Chu, L.M., Chung, C.-L., Mohd Farid, A., Hattori, T., Huang, Y.-C.,Kwan, H.S., Lam, R.Y.C., Lee, H.-H., Leung, M.W.K., Lee, S.S., Liou, R.-F.,Sahashi, N., Schlub, R.L., Shuey, L., Tang, A.M.C., Tsai, J.-N., Cannon, P.G.,Klopfenstein, N.B., Phylogenetic and population analyses of the invasive brown root-rot pathogen (Phellinus noxius) highlights the existence of three distinct populations with unique climate habitats. Eur. J. Plant Pathol. https:// doi.org/10.1007/s10658-019-01926-5 (In press).
Stewart, J.E., Kim, M.-S., Klopfenstein, N.B., 2018. Molecular genetic approaches toward understanding forest-associated fungi and their interactive roles within forest ecosystems. For. Pathol. Curr. For. Rep. https://doi.org/10.1007/s40725-018-0076-5.
Staton, E., 2018. Sestaton/Hmmer2Go: Hmmer2Go Version 0.17.8. Zenodo. https://doi.org/10.5281/zenodo.592436.
Subramanian, V., Yadav, J.S., 2008. Regulation and heterologous expression of P450 enzyme system components of the white rot fungus *Phanerochaete chrysosporium*. Enzym. Microb. Technol. 43 (2), 205–213. https://doi.org/10.1016/j.enzmictec.2007.09.001.
Syed, K., Yadav, J.S., 2012. P450 monooxygenases (P450ome) of the model white rot fungus *Phanerochaete chrysosporium*. Crit. Rev. Microbiol. 38 (4), 339–363. https://doi.org/10.3109/1040841X.2012.682050.
Ter-Hovhannisyan, V., Lomsadze, A., Chernoff, Y., Borodovsky, M., 2008. Gene prediction in novel fungal genomes using an ab initio algorithm with unsupervised training. Genome Res. 18, 1979–1990.
The CAZypedia Consortium, 2018. Ten years of CAZypedia: a living encyclopedia of carbohydrate-active enzymes. Glycobiology 28 (1), 3–8. https://doi.org/10.1093/glycob/cwx089.
Trapnell, C., Roberts, A., Goff, L., Pertea, G., Kim, D., Kelley, D.R., Pimentel, H., Salzberg, S.L., Rinn, J.L., Pachter, L., 2014. Differential gene and transcript expression analysis of RNA-seq experiments with TopHat and Cufflinks. Nat. Protoc. 7 (3), 562–579.
Tsai, J.-N., Ann, P.-J., Liou, R.-F., Hsieh, W.-H., Ko, W.-H., 2017. *Phellinus noxius*: molecular diversity among isolates from Taiwan and its phylogenetic relationship with other species of *Phellinus* based on sequences of the ITS region. Bot. Stud. 58, 9.
Urban, M., Cuzick, A., Rutherford, K., Irvine, A., Pedro, H., Pant, R., Sadanadan, V., Khamari, L., Billal, S., Mohanty, S., Hammond-Kosack, K.E., 2017. PHI-base: a new interfase and further directions for the multi-species pathogen-host interactions database. Nucleic Acids Res. 45 (D1), D604–D610.
Yin, Y., Mao, X., Yang, J., Chen, X., Mao, F., Xu, Y., 2012. dbCAN: a web resource for automated carbohydrate-active enzyme annotation. Nucleic Acids Res. 40 (W1), W445–W451.
Zaharia, M., Bolosky, W.J., Curtis, K., Fox, A., Patterson, D., Shenker, S., Stoica, I., Karp, R.M., Sittler, T., 2011. Faster and more accurate sequence alignment with SNAP. arXiv. 1111 5572. https://arxiv.org/abs/1111.5572v1.